

# Molecular Basis of Phospholipase A<sub>2</sub> Inhibition by Petrosaspongiolide M

In memory of Guido Sodano

Fabrizio Dal Piaz,<sup>[b]</sup> Agostino Casapullo,<sup>[a]</sup> Antonio Randazzo,<sup>[c]</sup> Raffaele Riccio,<sup>[a]</sup> Piero Pucci,<sup>[b]</sup> Gennaro Marino,<sup>[b]</sup> and Luigi Gomez-Paloma\*<sup>[a]</sup>

*Petrosaspongiolide M (PM) is an anti-inflammatory marine metabolite that displays a potent inhibitory activity toward group II and III secretory phospholipase A<sub>2</sub> (PLA<sub>2</sub>) enzymes. The details of the mechanism, which leads to a covalent adduct between PLA<sub>2</sub> and  $\gamma$ -hydroxybutenolide-containing molecules such as PM, are still a matter of debate. In this paper the covalent binding of PM to bee venom PLA<sub>2</sub> has been investigated by mass spectrometry and molecular modeling. The mass increment observed for the PM–PLA<sub>2</sub> adduct is consistent with the formation of a Schiff base by reaction of a PLA<sub>2</sub> amino group with the hemiacetal function (masked aldehyde) at the C-25 atom of the PM  $\gamma$ -hydroxybutenolide ring. Proteolysis of the modified PLA<sub>2</sub> by the endoprotease LysC followed by HPLC MS analysis allowed us to establish that the PLA<sub>2</sub>  $\alpha$ -amino terminal group of the Ile-1 residue was the only covalent binding site for PM. The stoichiometry of the reaction between PM and PLA<sub>2</sub> was also monitored and results showed that even with excess inhibitor, the prevalent product is a 1:1 (inhibitor:enzyme) adduct, although a 2:1 adduct is present as a minor component.*

*The 2:1 adduct was also characterized, which showed that the second site of reaction is located at the  $\epsilon$ -amino group of the Lys-85 residue. Similar results in terms of the reaction profile, mass increments, and location of the PLA<sub>2</sub> binding site were obtained for manoalide, a paradigm for irreversible PLA<sub>2</sub> inhibitors, which suggests that the present results may be considered of more general interest within the field of anti-inflammatory sesterterpenes that contain the  $\gamma$ -hydroxybutenolide pharmacophore. Finally, a 3D model, constrained by the above experimental results, was obtained by docking the inhibitor molecule into the PLA<sub>2</sub> binding site through AFFINITY calculations. The model provides an interesting insight into the PM–PLA<sub>2</sub> inhibition process and may prove useful in the design of new anti-inflammatory agents that target PLA<sub>2</sub> secretory enzymes.*

## KEYWORDS:

anti-inflammatory compounds · enzymes · inhibitors · mass spectrometry · natural products

## Introduction

Sesterterpenes of marine origin that contain the  $\gamma$ -hydroxybutenolide moiety have been studied for their potent anti-inflammatory activity since the discovery in 1980 of manoalide<sup>[1]</sup> (MLD, **1**, Scheme 1), which can be considered the reference compound within this class of bioactive natural products. Since then, many other related molecules have been isolated, such as seco-manoalide,<sup>[2]</sup> luffariellolides,<sup>[3]</sup> luffariellins,<sup>[4]</sup> luffolide,<sup>[5]</sup> cacospongionolides,<sup>[6]</sup> and recently petrosaspongiolides M-R,<sup>[7]</sup> all of which are capable of irreversible inhibition of PLA<sub>2</sub>. Among these compounds, petrosaspongiolide M (PM, **2**) has been the subject of detailed in vitro and in vivo pharmacological investigation. PM shows an IC<sub>50</sub> value of 0.6  $\mu$ M toward bee venom PLA<sub>2</sub> (MLD has an IC<sub>50</sub> value of 7.5  $\mu$ M under the same conditions),<sup>[7, 8]</sup> it is able to reduce the levels of prostaglandin E<sub>2</sub>, tumor necrosis factor  $\alpha$ , and leucotriene B<sub>4</sub> in a dose-dependent fashion,<sup>[9]</sup> and it has been shown to modulate the expression of inducible cyclooxygenase and nitric oxide synthetase by interference with the nuclear factor  $\kappa$ B.<sup>[10]</sup> Since PM shows no significant side effects that act on gastric mucosa at 10 mg Kg<sup>-1</sup> and is orally administrable, there is considerable interest in the design of simplified analogues of this molecule as new potential

candidates for the treatment of acute and/or chronic inflammation.

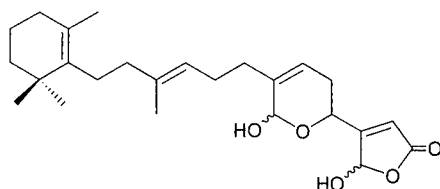
A number of investigations on the molecular aspects of PLA<sub>2</sub> inactivation by  $\gamma$ -hydroxybutenolide-containing molecules and in particular by MLD (**1**) have been reported. These investigations included biomimetic studies on the reaction of MLD with amino acids and peptides,<sup>[11]</sup> structure–activity relationships,<sup>[12]</sup>

[a] Prof. L. Gomez-Paloma, Dr. A. Casapullo, Prof. R. Riccio  
Dipartimento di Scienze Farmaceutiche  
via Ponte don Melillo  
Università degli Studi di Salerno  
84084 Fisciano, SA (Italy)  
Fax: (+ 39) 89-962828  
E-mail: gomez@unisa.it

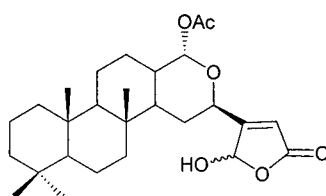
[b] Dr. F. Dal Piaz, Prof. P. Pucci, Prof. G. Marino  
Dipartimento di Chimica Organica e Biochimica  
Università di Napoli "Federico II"  
via Cinthia 6, 80126 Napoli (Italy)

[c] Dr. A. Randazzo  
Dipartimento di Chimica delle Sostanze Naturali  
Università degli Studi di Napoli "Federico II"  
via D. Montesano 49, 80131 Napoli (Italy)

ILE<sub>1</sub> ILE TYR PRO GLY<sub>5</sub> THR LEU TRP CYS GLY<sub>10</sub> HIS GLY ASN **LYS** SER<sub>15</sub>  
 SER GLY PRO ASN GLU<sub>20</sub> LEU GLY ARG PHE **LYS**<sub>25</sub> HIS THR ASP ALA CYS<sub>30</sub>  
 CYS ARG THR HIS ASP<sub>35</sub> MET CYS PRO ASP VAL<sub>40</sub> MET SER ALA GLY GLU<sub>45</sub>  
 SER **LYS** HIS GLY LEU<sub>50</sub> THR ASN THR ALA SER<sub>55</sub> HIS THR ARG LEU SER<sub>60</sub>  
 CYS ASP CYS ASP ASP<sub>65</sub> **LYS** PHE TYR ASP CYS<sub>70</sub> LEU **LYS** ASN SER ALA<sub>75</sub>  
 ASP THR ILE SER SER<sub>80</sub> TYR PHE VAL GLY **LYS**<sub>85</sub> MET TYR PHE ASN LEU<sub>90</sub>  
 ILE ASP THR **LYS** CYS<sub>95</sub> TYR **LYS** LEU GLU HIS<sub>100</sub> PRO VAL THR GLY CYS<sub>105</sub>  
 GLY GLU ARG THR GLU<sub>110</sub> GLY ARG CYS LEU HIS<sub>115</sub> TYR THR VAL ASP **LYS**<sub>120</sub>  
 SER **LYS** PRO **LYS** VAL<sub>125</sub> TYR GLN TRP PHE ASP<sub>130</sub> LEU ARG **LYS** TYR<sub>134</sub>



Manoalide (1)



Petrosaspongiolide M (2)

**Scheme 1.** The amino acid sequence of bee venom phospholipase A<sub>2</sub> (PLA<sub>2</sub>) and the chemical structures of manoalide and petrosaspongiolide M.

evidence that human-synovial PLA<sub>2</sub> was also irreversibly inactivated by MLD,<sup>[13]</sup> and a tentative location of the MLD binding site on bee venom PLA<sub>2</sub> at the ε-amino group of the Lys-88 residue.<sup>[14]</sup> When the location of the binding site was performed an incorrect sequence of PLA<sub>2</sub> was available (notably, in the correct sequence there is no Lys-88 residue, see Scheme 1).<sup>[15]</sup> Studies on the reaction mechanism were also undertaken and provided evidence for a nucleophilic attack by an amino group (for example, an ε-amino group of a Lys residue) on the hemiacetal function(s), or masked aldehydes, at the C-25 and C-24 atoms of MLD, which results in the formation of imine(s) termed Schiff bases.<sup>[16]</sup> Molecular modeling studies on the MLD–PLA<sub>2</sub> interaction that lead to the proposal of the Lys-94 residue as the best candidate for the imine formation have also been reported.<sup>[17]</sup> According to this model, the polar tail of MLD (1) interacts with a cationic site that consists of the Arg-58 and Lys-94 residues, whereas its hydrophobic core lies in a cleft defined by two β sheets in the C-terminal region of the enzyme. Overall, the wealth of research activity fostered by this family of natural products has indicated that their chemical mechanism of action is still a matter of debate. In this paper we report a detailed structural study of the inhibition of bee venom PLA<sub>2</sub> by PM (2) and MLD (1).

## Results and Discussion

Our study consisted of four main goals: a) determination of the nature and stoichiometry of the covalent binding of PM to PLA<sub>2</sub>, aimed at understanding the chemical inactivation mechanism; b) location on the PLA<sub>2</sub> protein of the PM covalent binding site(s); c) extension of the study to the case of MLD; d) construction of a suitable 3D structural model of the PM–PLA<sub>2</sub>

interaction by using our results as input data. Accordingly, from an experimental point of view the work can be divided into the following steps: a) comparative mass spectrometry analysis of the intact and covalently modified PLA<sub>2</sub> species; b) proteolytic digestion of both the free and inhibitor-bound protein samples followed by HPLC purification and mass spectrometry analysis of the fragments that result; c) molecular modeling of the inhibitor–PLA<sub>2</sub> complex.

All the experiments were initially applied to the study of PLA<sub>2</sub> inhibition by PM and, after careful adjustment of the experimental conditions, a parallel set of experiments was performed to investigate the mode of action of MLD and thus allow a comparison of the data to be made and the proposed model of PLA<sub>2</sub> inactivation to be put on a more firm and general ground.

### Chemical mechanism of covalent inhibition of PLA<sub>2</sub> by PM

Bee venom PLA<sub>2</sub> was incubated with a 1–5 molar excess of PM at 40 °C for 5 min in an Na<sub>2</sub>B<sub>4</sub>O<sub>7</sub> buffer solution (10 mM, pH 7.4). The mixture was treated with excess NaBH<sub>4</sub> in order to selectively reduce the Schiff base (imine) conceivably formed during the incubation. This step allowed us to overcome the inherent instability of the Schiff bases during MS analysis. The NaBH<sub>4</sub> reaction products were then fractionated by reversed-phase (RP) HPLC (Figure 1) and identified by electrospray mass spectrometry (ESMS). Four major species were detected in the chromatogram and identified. These species consisted of unreacted PLA<sub>2</sub> with one or two oxidized Met (ox-Met) species (peaks 1 and 2, respectively, Figure 1), a monomodified (peak 3) and a dimodified (peak 4) PLA<sub>2</sub> species. The ESMS analysis of the inhibitor-bound PLA<sub>2</sub> samples showed mass values of 16594.7 ± 1.6 Da and 17039.1 ± 1.5 Da, which corresponds to an increase com-

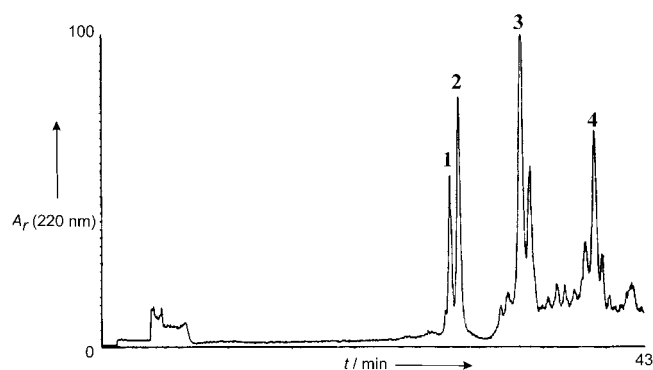


**Figure 1.** RP HPLC chromatogram of the separation of PM/PLA<sub>2</sub> reaction products. A<sub>r</sub>(220 nm) is the relative absorbance at 220 nm. Mass spectrometry analyses of each fraction are reported in Table 1.

pared to unreacted PLA<sub>2</sub> of 444 Da and 888 Da for the mono- and dimodified PLA<sub>2</sub> forms, respectively (molecular weight of intact PLA<sub>2</sub> = 16 150.1 ± 1.6 Da; Table 1). Hence, molecular mass differences detected between reacted and unreacted PLA<sub>2</sub> species were very informative with regard to the stoichiometry of the modifications and revealed that the most relevant reaction product in these conditions is a 1:1 covalent PM–PLA<sub>2</sub> adduct, which occurs along with a 2:1 complex minor product. MS data

**Table 1.** Mass spectrometry analysis of PM/PLA<sub>2</sub> reaction products.<sup>[a]</sup>

Fraction	Measured mass [Da]	Description of the species	Expected molecular mass [Da]
1	16166.3 ± 1.3	PLA <sub>2</sub> (2 Met ox) Hex NAc <sub>2</sub> Hex <sub>2</sub>	16166.4
	16328.4 ± 1.4	PLA <sub>2</sub> (2 Met ox) Hex NAc <sub>2</sub> Hex <sub>3</sub>	16328.6
	16490.8 ± 0.9	PLA <sub>2</sub> (2 Met ox) Hex NAc <sub>2</sub> Hex <sub>4</sub>	16490.8
2	16150.1 ± 1.6	PLA <sub>2</sub> (1 Met ox) Hex NAc <sub>2</sub> Hex <sub>2</sub>	16150.3
	16311.9 ± 1.1	PLA <sub>2</sub> (1 Met ox) Hex NAc <sub>2</sub> Hex <sub>3</sub>	16312.5
	16475.0 ± 1.5	PLA <sub>2</sub> (1 Met ox) Hex NAc <sub>2</sub> Hex <sub>4</sub>	16474.7
3	16594.7 ± 1.6	PLA <sub>2</sub> (1 Met ox) Hex NAc <sub>2</sub> Hex <sub>2</sub> + PM	16594.8
	16755.8 ± 1.3	PLA <sub>2</sub> (1 Met ox) Hex NAc <sub>2</sub> Hex <sub>3</sub> + PM	16757.0
	16918.9 ± 0.9	PLA <sub>2</sub> (1 Met ox) Hex NAc <sub>2</sub> Hex <sub>4</sub> + PM	16919.2
4	17039.1 ± 1.5	PLA <sub>2</sub> (1 Met ox) Hex NAc2 Hex <sub>2</sub> + 2PM	17039.3
	17202.3 ± 1.1	PLA <sub>2</sub> (1 Met ox) Hex NAc2 Hex <sub>3</sub> + 2PM	17201.5
	17362.5 ± 1.3	PLA <sub>2</sub> (1 Met ox) Hex NAc2 Hex <sub>4</sub> + 2PM	17363.7

[a] Fraction numbers are indicated in Figure 1.

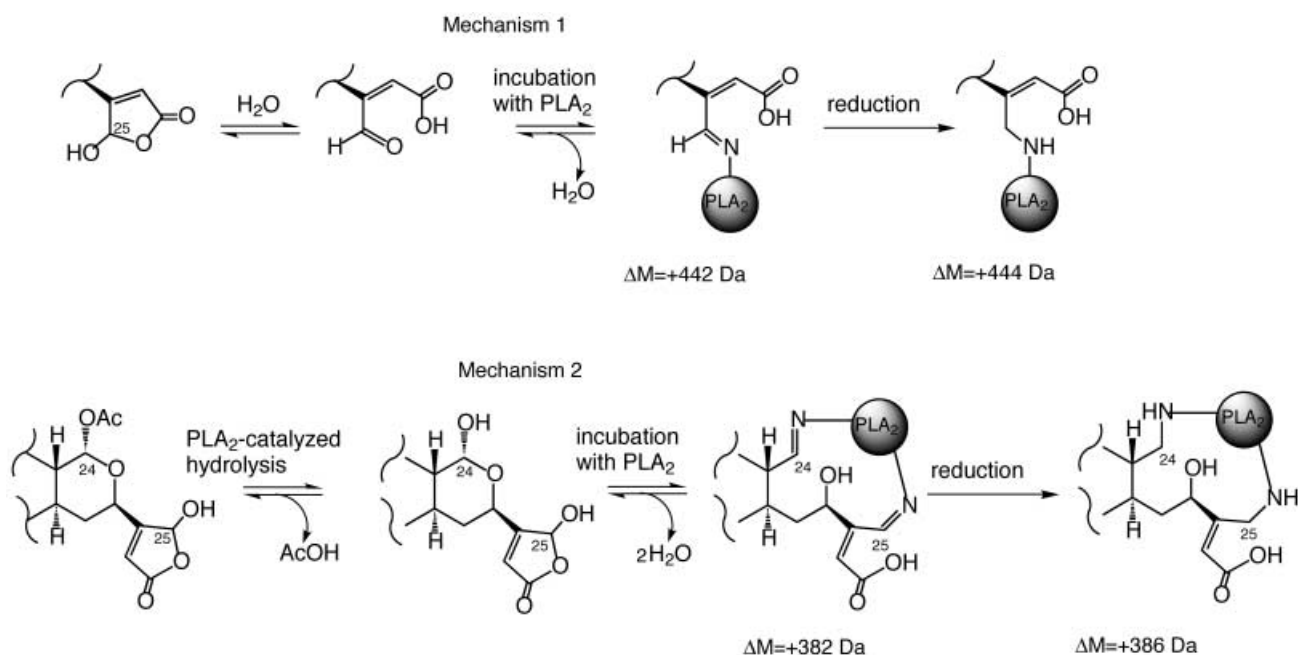
were also used to address one of the most crucial points in the study of the chemical mechanism that lies behind PLA<sub>2</sub> inactivation by PM and related molecules, which allowed us to propose a detailed reaction pathway fully consistent with all the experimental evidence (see below). Such a proposal in turn requires an accurate analysis of all the reactive centers of the inhibitor molecule. Although several possibilities arise when a nucleophilic attack by a PLA<sub>2</sub> amino group at an electrophilic site of the sesterterpene **2** is considered, some of these possibilities (such as a Michael addition to the conjugate ester carbonyl in the butenolide moiety) can be ruled out by taking into account literature data.<sup>[16]</sup> This process leaves the formation of an imine from a hemiacetal/aldehyde as the only mechanism in agreement with all the experimental evidence collected so far. Chemical evidence that (reversible) formation of an imine is the key step in the inactivation pathway was obtained by treatment of a sample of PLA<sub>2</sub> preincubated with PM with a hydroxylamine solution (1:10 molar ratio of protein to hydroxylamine) for 5 minutes to yield the corresponding PM oxime and release the free (and active) form of PLA<sub>2</sub>. HPLC and ESMS analysis of the reaction mixture that results showed the presence of only the unmodified protein species, which supports imine formation.<sup>[16]</sup> A parallel experiment was performed in which hydroxylamine was added to the PM–PLA<sub>2</sub> reaction product after reduction with NaBH<sub>4</sub>. As expected, in this case LC–MS detected a mixture of mono- and dimodified PLA<sub>2</sub> species, much like that seen in the case of simple PM–PLA<sub>2</sub> incubation.

However, a further complication stems from the presence in the PM molecule (as well as other related inhibitors) of two reactive sites, that is, C-25 and C-24 hemiacetal groups. Even if in

the specific case of PM the C-24 hemiacetal group is present as an acetyl derivative and therefore much less sensitive to nucleophilic attack, since PLA<sub>2</sub> may work as a generic esterase a reactivation of this functionality by a PLA<sub>2</sub>-catalyzed hydrolysis of the acetate in a sort of a suicide mechanism remains a possibility. The mass increment of 444 Da observed for the monomodified PLA<sub>2</sub> species (after NaBH<sub>4</sub> reduction and hence corresponding to a  $\Delta M_{\text{bound-free}}$  of 442 Da) allowed us to discriminate between two reaction mechanisms that may be postulated on the basis of the previous considerations (Scheme 2). The expected mass increments (after NaBH<sub>4</sub> reduction) for the two putative reaction pathways for PM–PLA<sub>2</sub> inactivation are 444 Da for a single Schiff base formation at the C-25 atom in the butenolide ring of PM and 386 Da for a bidentate mode of binding, which requires the PLA<sub>2</sub>-catalyzed deacetylation of PM at the C-24 atom followed by formation of two imines at the C-24 (pyran ring) and C-25 (butenolide ring) positions (Scheme 2). Therefore, our data indicate that the  $\gamma$ -hydroxybutenolide is the only structural element required for PLA<sub>2</sub> covalent inhibition, which rules out a prominent role for the pyrane ring previously thought<sup>[16]</sup> to be the other key element actively involved in the irreversible modification of the enzyme.

#### Location of binding site(s)

Identification of the inhibitor binding site(s) on PLA<sub>2</sub> was performed through the following protocol: Unreacted, monomodified, and dimodified PLA<sub>2</sub> forms previously isolated by RP HPLC on a Vydak C4 analytical column were subjected to disulfide bridge reduction with guanidinium chloride (GndCl) and dithiothreitol (DTT) (50:1 molar excess with respect to the protein), SH group alkylation (iodoacetamide in 10:1 molar excess to the protein), and then enzymatic hydrolysis. The endoprotease LysC, which cleaves peptide bonds adjacent to lysine residues, was used as a proteolytic agent to locate the putative reactive lysine residues. The peptide mixture so obtained was then analyzed by LC–MS. Hydrolysis of the intact protein (Figure 2A) allowed us to obtain a full LysC peptide map of the PLA<sub>2</sub> amino acid sequence that was used as a reference for the experiments on the modified PLA<sub>2</sub> species. Excellent agreement was observed between the measured and expected mass values for all the peptides (Table 2). When the same procedure was performed on the monomodified protein (Figure 2B), two differences were observed in the HPLC chromatogram. The N-terminal glycopeptide (residues 1–14) disappeared (peak 8, Figure 2) and a new peak characterized by a higher retention time simultaneously appeared (peak 11, Figure 2). It is important to point out that the residue 1–14 peptide fragment contains the PLA<sub>2</sub> glycosylation site at the Asn-13 residue and bears two different glycoforms. The ESMS spectrum of this fraction, which displays molecular masses of 2953.3 ± 0.7 and 3115.7 ± 0.2 Da, is consistent with that expected for peptide 1–14 covalently linked to the PM molecule (all masses are 444 Da higher than those of the same peptide observed in the unreacted glycoprotein). The presence of the modified 1–14 glycopeptide and the absence of any other modified peptide indicate that the monomodified PLA<sub>2</sub> adduct consists of a homogeneous species



**Scheme 2.** The two mechanisms postulated for the PM–PLA<sub>2</sub> inactivation reaction and the expected mass increments. The experimentally observed mass increment was 444 Da (after NaBH<sub>4</sub> reduction), which supports Mechanism 1.

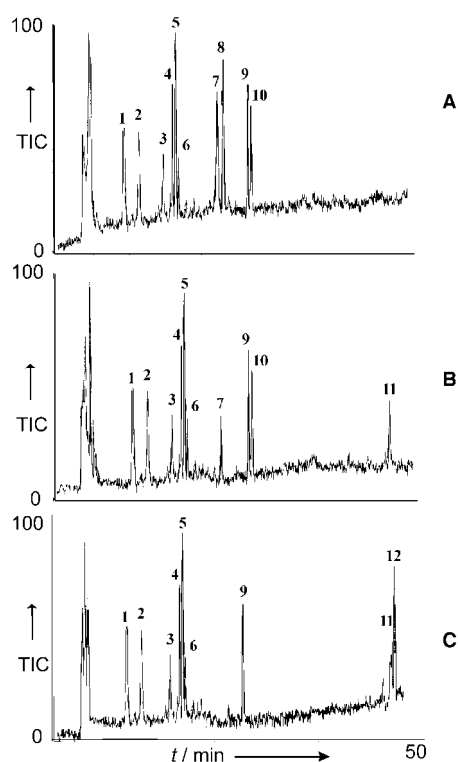


**Table 2.** Mass spectrometry analysis of the peptide mixture that results from LysC hydrolysis of unmodified, monomodified, and dimodified PLA<sub>2</sub> (after reaction with PM or MLD).<sup>[a]</sup>

Fraction	Measured mass [Da]	Description of the peptide	Expected molecular mass [Da]
1	2187.2 ± 0.2	48–66	2187.1
2	2581.6 ± 0.3	26–47 (1 Met ox)	2581.7
3	2565.7 ± 0.1	26–47	2565.7
4	3165.6 ± 0.6	95–120	3166.0
5	1190.8 ± 0.2	15–25	1191.3
6	3014.3 ± 0.8	48–72	3015.6
7	1143.9 ± 0.5	86–94	1144.1
8	2507.8 ± 0.8	1–14 + Hex NAc <sub>2</sub> Hex <sub>2</sub>	2508.1
9	2670.2 ± 0.7	1–14 + Hex NAc <sub>2</sub> Hex <sub>3</sub>	2670.3
10	1417.2 ± 0.6	125–134	1416.8
11	1387.7 ± 0.4	73–85	1388.1
	2953.3 ± 0.7	1–14 + Hex NAc <sub>2</sub> Hex <sub>2</sub> + PM	2952.6
	3115.7 ± 0.2	1–14 + Hex NAc <sub>2</sub> Hex <sub>3</sub> + PM	3114.8
11 b	2909.0 ± 0.5	1–14 + Hex NAc <sub>2</sub> Hex <sub>2</sub> + MLD	2908.6
	3071.6 ± 0.8	1–14 + Hex NAc <sub>2</sub> Hex <sub>3</sub> + MLD	3070.8
12	2958.7 ± 0.2	73–94 + 2 PM	2958.8
12 b	2915.2 ± 0.6	73–94 + 2 MLD	2914.4

[a] Fraction numbering is consistent with Figure 2 and Figure 4. The numbers used for the peptide descriptions correspond to the residue numbers in Scheme 1.

**Figure 2.** LC–MS analysis of unmodified (A), monomodified (B) and dimodified (C) PLA<sub>2</sub> enzymes after reaction with PM and digestion by endoprotease LysC. TIC = relative total ion current. Mass spectrometry results are summarized in Table 2.

that contains a single molecule of PM covalently bound to the PLA<sub>2</sub> N terminus (that is, the NH<sub>2</sub> group of the Ile-1 residue; see Scheme 1). In principle, the ε-amino group at the Lys-14 residue is another potential binding site present in the 1–14 fragment.

However, this possibility was ruled out since no differences were detected in the efficiency of LysC hydrolysis at the Lys-14/Ser-15 peptide linkage in the unmodified and modified PLA<sub>2</sub>, a finding in conflict with the presence of such a sterically demanding molecule at this Lys residue. The identification of the PLA<sub>2</sub> N terminus as virtually the only covalent PM binding site led us to speculate on the possible origin of such a high binding

specificity. A noncovalent PM–PLA<sub>2</sub> recognition process is very likely to take place prior the covalent inactivation process. As can be appreciated from visual inspection of the crystallographic coordinates of bee venom PLA<sub>2</sub>, a peculiar feature of its tertiary structure is the folding of the N terminus back onto the pocket that leads to the catalytic site. This unusual structural arrangement is clearly relevant for the inhibition of PLA<sub>2</sub> catalytic activity (see below).

The two sites of covalent modification in the 2:1 PM–PLA<sub>2</sub> adduct were identified by means of a protocol very similar to that described above (Figure 2C). The results are consistent with one binding site within the 1–14 peptide fragment (as in the case of 1:1 adduct) and a second one located at the Lys-85 residue. Indeed, the fractions corresponding to the PLA<sub>2</sub> fragments that consist of residues 73–85 and 86–94 (peaks 7 and 10, respectively, Figure 2C) disappeared from the chromatogram and a new peak was observed (fraction 13) whose ESMS analysis was in agreement with that expected for the peptide fragment that contains residues 73–94 bound to one PM molecule. It should be emphasized that the presence of the inhibitor molecule at the Lys-85 residue prevented catalysis of the hydrolysis of the peptide bond between residues 85 and 86 by LysC. Thus, the 2:1 inhibitor–enzyme adduct also appeared to be a homogeneous species that contains one molecule of PM bound to the N terminus (the amino group of the Ile-1 residue) and a second molecule of PM linked to the ε-amino group of the Lys-85 residue.

### PLA<sub>2</sub> inhibition by MLD

The above-described experimental procedure was applied to the case of MLD–PLA<sub>2</sub> inhibition to attempt to put our results in a broader perspective and to test the scope and the frame of validity of our model. Remarkably, the results obtained in this last set of experiments were in all respects equivalent to those previously described for the PM molecule. The MLD–PLA<sub>2</sub> reaction also proceeds in a few minutes and leads to a major monomodified and a minor dimodified protein species product (Figure 3 and Table 3). Again the measured PLA<sub>2</sub> mass increments  $\Delta M_{\text{bound-free}}$  were of pivotal importance in the determination of the chemical mechanism involved in the enzyme

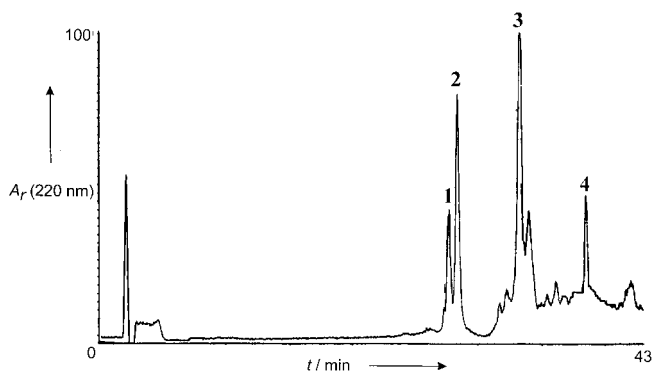


**Figure 3.** RP HPLC chromatogram of the separation of MLD/PLA<sub>2</sub> reaction products. Mass spectrometry analyses of the fractions are reported in Table 3.

Fraction	Measured mass [Da]	Description of the species	Expected molecular mass [Da]
1	16 166.8 ± 1.1	PLA <sub>2</sub> (2 Met ox) Hex NAC <sub>2</sub> Hex <sub>2</sub>	16 166.4
	16 328.5 ± 1.0	PLA <sub>2</sub> (2 Met ox) Hex NAC <sub>2</sub> Hex <sub>3</sub>	16 328.6
	16 490.7 ± 1.3	PLA <sub>2</sub> (2 Met ox) Hex NAC <sub>2</sub> Hex <sub>4</sub>	16 490.8
2	16 150.3 ± 1.6	PLA <sub>2</sub> (1 Met ox) Hex NAC <sub>2</sub> Hex <sub>2</sub>	16 150.3
	16 312.9 ± 0.9	PLA <sub>2</sub> (1 Met ox) Hex NAC <sub>2</sub> Hex <sub>3</sub>	16 312.5
	16 474.3 ± 1.8	PLA <sub>2</sub> (1 Met ox) Hex NAC <sub>2</sub> Hex <sub>4</sub>	16 474.7
3	16 551.0 ± 1.6	PLA <sub>2</sub> (1 Met ox) Hex NAC <sub>2</sub> Hex <sub>2</sub> + MLD	16 550.8
	16 713.0 ± 1.2	PLA <sub>2</sub> (1 Met ox) Hex NAC <sub>2</sub> Hex <sub>3</sub> + MLD	16 713.0
	16 874.9 ± 1.0	PLA <sub>2</sub> (1 Met ox) Hex NAC <sub>2</sub> Hex <sub>4</sub> + MLD	16 875.2
4	16 950.5 ± 1.8	PLA <sub>2</sub> (1 Met ox) Hex NAC <sub>2</sub> Hex <sub>2</sub> + 2 MLD	16 951.3
	17 112.6 ± 1.7	PLA <sub>2</sub> (1 Met ox) Hex NAC <sub>2</sub> Hex <sub>3</sub> + 2 MLD	17 113.5
	17 274.8 ± 1.0	PLA <sub>2</sub> (1 Met ox) Hex NAC <sub>2</sub> Hex <sub>4</sub> + 2 MLD	17 275.7

[a] Fraction numbers are indicated in Figure 1.

inactivation process (Table 2). Even the results of the experiments for the location of the MLD binding site(s) nicely matched those of the related PM molecule and support covalent modifications at the N terminus for the 1:1 adduct and at both the N terminus and the Lys-85 residue for the 2:1 adduct (Figure 4). It is noteworthy that the MLD molecule displays two reactive electrophilic centers, namely the C-24 (in the pyran ring) and C-25 (in the γ-hydroxybutenolide ring) free hemiacetal groups. Nevertheless, we again detected no bidentate mode of binding of MLD to PLA<sub>2</sub> (that is, two nucleophilic attacks at the

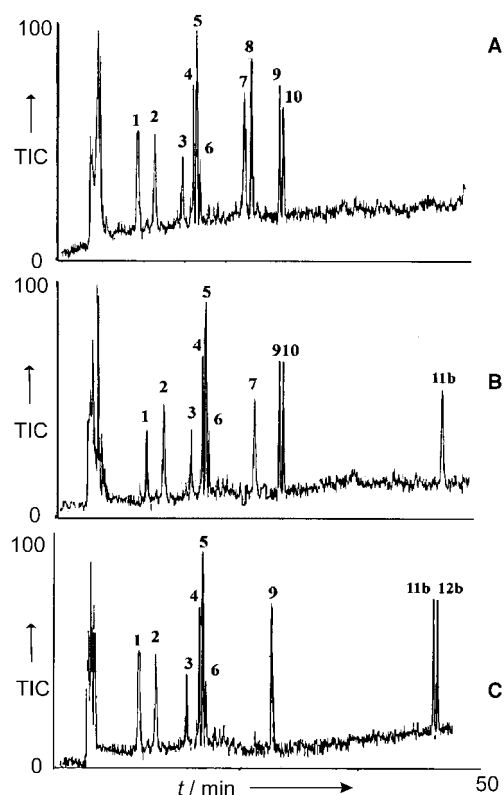


**Figure 4.** LC–MS analysis of unmodified (A), monomodified (B) and dimodified (C) PLA<sub>2</sub> enzymes after reaction with MLD and digestion by endoprotease LysC. Mass spectrometry results are summarized in Table 2.

C-24 and C-25 atoms) since all MS data are fully consistent with the exclusive involvement of the C-25 hemiacetal function in the butenolide moiety of MLD. Before direct evidence for the exact nature of chemical modification that occurs in MLD upon binding to PLA<sub>2</sub> was available, the possibility that two Lys residues spatially or sequentially close to each other would deliver a nucleophilic attack to both MLD reaction centers was long considered a valid hypothesis,<sup>[16]</sup> particularly since PLA<sub>2</sub> contains a segment with the sequence Lys<sub>94</sub>-Cys<sub>95</sub>-Tyr<sub>96</sub>-Lys<sub>97</sub>. On the other hand, since this bidentate binding appears not to occur, the pyran ring could well be involved in the inhibitor–enzyme recognition process at a different level, for instance it may participate in the formation of favorable noncovalent interactions (see below).

### Molecular modeling studies

The final step in this study concerned the construction of a 3D model of the PM–PLA<sub>2</sub> complex. We aimed to achieve a better understanding of the enzyme inactivation process at a molecular level to shed more light on the origin of the remarkable specificity (in terms of a noncovalent binding site) observed for these molecules. All the molecular modeling work was performed on the crystallographic structure of bee venom PLA<sub>2</sub> with a phospholipid transition state analogue in its active site (Protein Databank (PDB) code 1POC).<sup>[18]</sup> The phospholipid analogue was then taken away from the active site and replaced with the PM molecule. The docking procedure was performed by using the AFFINITY module of the INSIGHT II (version 1998) suite of software (Accelrys Inc., San Diego). This software module allows a conformational grid search to maximize the favorable interactions (Van der Waals, electrostatic, and hydrogen bonds) between a drug and a receptor. This maximization is achieved by optimization of both sets of 3D coordinates of the drug (its conformation and positioning) and those of the protein active site, which is usually defined by a distance criterion. The experimental information on the location of the inhibitor covalent binding site was used to correctly orientate the PM molecule within the enzyme pocket. Accordingly, the polar tail of the inhibitor, which contains the reactive center ( $\gamma$ -hydroxybutenolide, ring E, Figure 5), faced the outer, solvent exposed surface of the protein towards the N-terminal residue, while the lipophilic tetracyclic system was located in the inner portion of the pocket. Once the PM molecule was placed in proximity to the catalytic site, AFFINITY calculations were performed. Adjustments of both the PM molecule and the PLA<sub>2</sub> active site were allowed and the active site was defined as a 7 Å sphere around the centroid of the PM molecule. The PM–PLA<sub>2</sub> complex was further optimized by standard molecular mechanics calculations by using the AMBER force field. The final model obtained after all these refinements is reported in Figure 5. Among the most convincing features of this model, we noticed the excellent shape complementarity of the hydrophobic core of the inhibitor (rings A, B, C, and D) and the protein surface delimiting the active site. It should be noted that in this orientation the PM C-25 hemiacetal carbon atom and the PLA<sub>2</sub> N terminus are found in close proximity, even though this distance was not forced by any

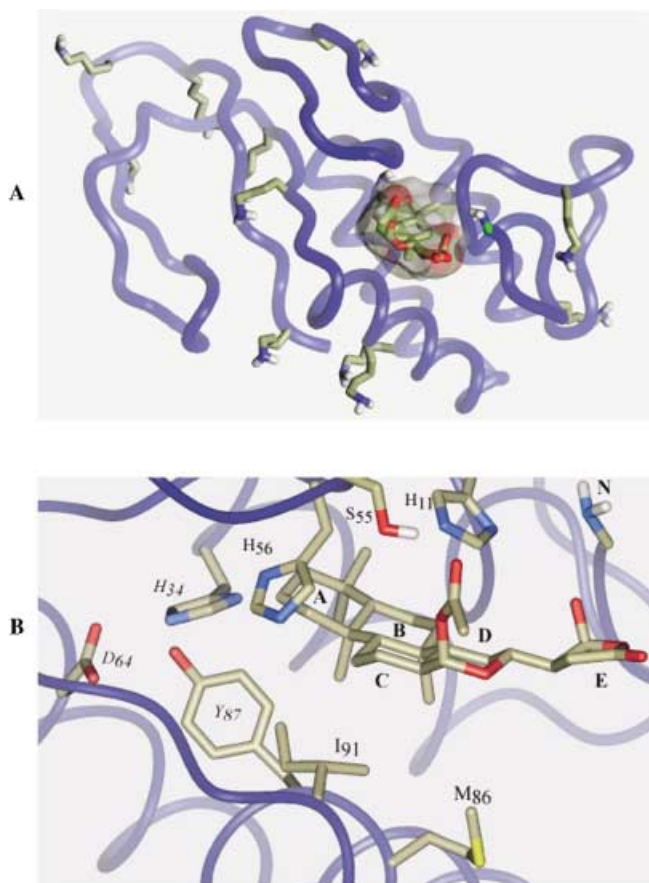


**Figure 5.** A) 3D model of the PM–PLA<sub>2</sub> adduct. The protein backbone is represented by a blue ribbon. Amino acid side chains are omitted for clarity, except for those of Lys residues and the N-terminal group. The PM molecule is displayed as a stick representation surrounded by a transparent solvent-accessible surface. B) Expanded view of the model to show the details of the interaction of PM with the PLA<sub>2</sub> active site. Color code: carbon, gold; oxygen, red; nitrogen, blue; hydrogen, white. Only heavy atoms are displayed, except for the S55 hydroxy group and the N-terminal groups.

sort of constraint during the calculations. Ring A atoms (C1–C4 and CH<sub>3</sub>-20 and CH<sub>3</sub>-21) lie in the vicinity of (about 3.0 Å away from) the Tyr-87 and His-34 residues, two of the three residues that compose the PLA<sub>2</sub> catalytic triad. The Asp-64 residue (the third residue actively involved in PLA<sub>2</sub> catalysis) is located further away from the inhibitor at a distance of about 5.0 Å. The inhibitor tetracyclic system appears to be literally sandwiched by several amino acid side chains. The His-56 and His-11 residues stack with the bottom ( $\alpha$ ) faces of ring A and ring B, respectively, whereas at the top ( $\beta$ ) face of the inhibitor the Met-86 side chain protrudes towards the Me-18 residue (rings C and D). Towards the outer side of the inhibitor, Tyr-87 and Ile-91 side chains make contacts with rings B and C, respectively. The Ser-55 hydroxy group is engaged in a hydrogen bond with the PM acetyl carbonyl group attached to the C-24 hemiacetal group in pyran ring D.

The model proved particularly useful in attempts to unravel the details of the mechanism of PLA<sub>2</sub> inactivation at the atomic level and strongly supports the view in which the initial event is a noncovalent recognition between PM and the enzyme, followed by nucleophilic attack by the PLA<sub>2</sub> N terminus at the C-25



butenolide hemiacetal group. Indeed, the recognition could be driven by a number of favorable interactions, such as Van der Waals or hydrophobic interactions (water molecules are likely to be released in the process) and probably H bond(s). These interactions would in turn ensure the correct positioning of the inhibitor within the binding pocket and thus bring the functional groups involved in the formation of the Schiff base within bonding distance of one another.

A structure-based rationalization of the formation of the dimodified species appears to be more complicated. On the one hand, the Lys-85 residue appears to be the second closest nitrogen nucleophile to the inhibitor molecule when it is in the binding pocket, whereas on the other hand the introduction of a second PM molecule into the PLA<sub>2</sub> active site appears to involve a rather large conformational rearrangement. A possible speculation based on the present model is that there could be additional room to accommodate a second inhibitor molecule in another region of the same pocket. This hypothesis would imply that the dimodified PLA<sub>2</sub> species contains two inhibitor molecules piled on top of each other and thus the large pocket delimited by the three  $\alpha$  helices of the enzyme is filled up completely. However, since it is hard to make reasonable predictions of the inhibitor-PLA<sub>2</sub> molar ratios under physiological conditions, the biological relevance of the 2:1 adduct is not clear at the present stage.

The overall picture reported in this paper may be instrumental in the design of simplified PM analogues as novel lead compounds for the treatment of acute and chronic inflammation.

## Experimental Section

**PLA<sub>2</sub> – inhibitor adduct analysis:** Bee venom PLA<sub>2</sub> (100  $\mu$ g, 6.2 nmol) was incubated in Na<sub>2</sub>B<sub>4</sub>O<sub>7</sub> solution (100  $\mu$ L; 10 mM, pH 7.4) in the presence of a 5:1 molar excess of inhibitor (PM) at 40 °C for 5 min. The resulting mixture was diluted with an equal volume of a NaBH<sub>4</sub> (3 mM) and Na<sub>2</sub>B<sub>4</sub>O<sub>7</sub> (10 mM) solution and incubated for 2 hours at 0 °C. The reduction reaction was quenched by addition of HCl (5  $\mu$ L, 6 M) and the reaction products were fractionated by RP HPLC on a C4 column. Modified glycoproteins were analyzed by means of a linear gradient from 25% to 95% of acetonitrile in 0.1% trifluoroacetic acid (TFA) over 35 min. Elution was monitored at 220 nm. Individual fractions were collected and identified by ESMS. Mass analysis was performed on an API100 single quadrupole spectrometer (Applied Biosystems) equipped with an electrospray ion source. Data were acquired and elaborated by using the Biolmultiviewer program (Applied Biosystems). Mass calibration was performed by means of multiply charged ions from a separate injection of horse heart myoglobin (Sigma; average molecular mass = 16951.5 Da). All masses are reported as average values.

**Reaction with hydroxylamine:** PLA<sub>2</sub> was first treated with PM as described above. After 5 minutes of incubation a hydroxylamine-containing solution was added to obtain a final hydroxylamine concentration of 0.6 mM (molar protein:hydroxylamine = 1:10) and the mixture was left to react for 2 hours at 40 °C. Reaction products were analyzed by RP HPLC and ESMS under the same conditions as previously described. The same procedure was also performed on the glycoprotein-inhibitor complex after a 2 hour reduction with NaBH<sub>4</sub>.

**Location of the binding site(s):** Unreacted, monomodified, and dimodified PLA<sub>2</sub> were purified by HPLC and individually underwent disulfide bond reduction. Each species was dissolved in tris(hydroxymethyl)aminomethane (Tris; 100 mM), ethylenediaminetetraacetate (EDTA; 1 mM), GndCl (6 M), and DTT (5 mM) at pH 7.5 and incubated under a nitrogen atmosphere for 2 hours at 37 °C. The free thiol groups obtained were alkylated by addition of an equal volume of a solution of Tris (100 mM), EDTA (1 mM), GndCl (6 M), and iodacetamide (50 mM) at pH 7.5. The alkylation reaction was allowed to proceed for 30 minutes in the dark at room temperature and was then quenched by HPLC injection.

Alkylated species were digested with the endoprotease LysC in ammonium bicarbonate (50 mM, pH 8.5) at 37.0 °C for 4 h at a 1:50 (w:w) LysC:protein ratio. Proteolytic fragments were analyzed by LC-MS performed on an API100 single quadrupole electrospray spectrometer (Applied Biosystems) equipped with two Perkin-Elmer Series 200 LC isocratic pumps. Chromatographic separation was carried out on a Phenomenex C18 column by means of a 40 min linear gradient from 15–55% acetonitrile in 2% formic acid and 0.1% TFA. Mass spectra were acquired in an *m/z* interval of 600–1800.

**Molecular modeling:** All molecular modeling was performed on a Silicon Graphics Indigo 2 workstation equipped with a R10000 processor. For AFFINITY calculations (InsightII version 1998, Accelrys, Inc., San Diego, USA) the CVFF force field was used with standard parameters. The 3D coordinates of PLA<sub>2</sub> were obtained from the PDB archive (<http://www.rcsb.org/pdb/>; PDB code for bee venom PLA<sub>2</sub> crystallographic structure: 1POC). The input PM-PLA<sub>2</sub> complex for the AFFINITY calculations was obtained by visual docking the PM molecule into the hydrophobic pocket of PLA<sub>2</sub>. Once the AFFINITY docking procedure was completed, a full energy minimization was carried out on the PM-PLA<sub>2</sub> complex by using the conjugate gradient algorithm until the maximum derivative was less than 0.1 Kcal.

*This paper is dedicated to the memory of Guido Sodano, a dear friend and colleague who passed away on June 7<sup>th</sup> 2001. We thank Maria Cristina Lavazzo for her contribution to this project during the preparation of her graduation thesis. We also thank Dr. Adele Cutignano for the help she provided while making her first steps towards learning mass spectrometry techniques. Financial support was provided by the Università di Salerno and Napoli "Federico II", Consiglio Nazionale delle Ricerche (CNR, Roma), and Ministero dell'Università e della Ricerca Scientifica e Tecnologica (MURST, Roma) through the PRIN 1999-2001 program. We are particularly grateful to the late Professor Guido Sodano for an authentic sample of manoalide.*

- [1] E. D. De Silva, P. J. Scheuer, *Tetrahedron Lett.* **1980**, 21, 1611–1612; for a review on marine PLA<sub>2</sub> inhibitors, see: B. C. M. Potts, D. J. Faulkner, R. S. Jacobs, *J. Nat. Prod.* **1992**, 55, 1701–1717.
- [2] E. D. De Silva, P. J. Scheuer, *Tetrahedron Lett.* **1981**, 22, 3147–3150.
- [3] K. F. Albizati, T. Holman, D. J. Faulkner, K. B. Glaser, R. S. Jacobs, *Experientia* **1987**, 43, 949–950.
- [4] M. R. Kernan, D. J. Faulkner, R. S. Jacobs, *J. Org. Chem.* **1987**, 52, 3081–3083.
- [5] M. R. Kernan, D. J. Faulkner, L. Parkanyi, J. Clardy, M. S. De Carvalho, R. S. Jacobs, *Experientia* **1989**, 45, 388–390.
- [6] a) S. De Rosa, S. De Stefano, N. Zavodnik, *J. Org. Chem.* **1988**, 53, 5020–5023; b) S. De Rosa, A. Crispino, A. De Giulio, C. Iodice, R. Pronzato, N. Zavodnik, *J. Nat. Prod.* **1995**, 58, 1776–1780.
- [7] A. Randazzo, C. Debitus, L. Minale, P. G. Pastor, M. J. Alcaraz, M. Payà, L. Gomez-Paloma, *J. Nat. Prod.* **1998**, 61, 571–575.

- [8] Much care must be taken with comparisons of IC<sub>50</sub> values of these PLA<sub>2</sub> irreversible blockers. IC<sub>50</sub> values may vary as much as 100-fold depending on how long the enzyme is preincubated with the inhibitor. Therefore, data are fully comparable only when measured under the same experimental conditions.
- [9] P. Garcia-Pastor, A. Randazzo, L. Gomez-Paloma, M. J. Alcaraz, M. Payà, *J. Pharmacol. Exp. Ther.* **1999**, *289*, 166–172.
- [10] I. Posadas, M. C. Terencio, A. Randazzo, L. Gomez-Paloma, M. J. Alcaraz, M. Payà, *J. Leukocyte Biol.* **2002**, submitted.
- [11] K. B. Glaser, R. S. Jacobs, *Biochem. Pharmacol.* **1987**, *36*, 2079–2086.
- [12] K. B. Glaser, M. S. De Carvalho, R. S. Jacobs, M. R. Kernan, D. J. Faulkner, *Mol. Pharmacol.* **1989**, *36*, 782–788.
- [13] P. B. Jacobson, L. A. Marshall, A. Sung, R. S. Jacobs, *Biochem. Pharmacol.* **1990**, *39*, 1557–1564.
- [14] K. B. Glaser, T. S. Vedvick, R. S. Jacobs, *Biochem. Pharmacol.* **1988**, *37*, 3639–3646.
- [15] K. Kuchler, M. Gmachl, M. J. Sippl, G. Kreil, *Eur. J. Biochem.* **1989**, *184*, 249–254; for a more recent account on PLA<sub>2</sub> enzymology, see: O. G. Berg, M. H. Gelb, M. D. Tsai, M. K. Jain *Chem. Rev.* **2001**, *101*, 2613–2653.
- [16] B. C. M. Potts, D. J. Faulkner, M. S. De Carvalho, R. S. Jacobs, *J. Am. Chem. Soc.* **1992**, *114*, 5093–5100.
- [17] A. R. Ortiz, M. T. Pisabarro, F. Gago, *J. Med. Chem.* **1993**, *36*, 1866–1879.
- [18] a) D. L. Scott, Z. Otwinowski, M. H. Gelb, P. B. Sigler, *Science*, **1990**, *250*, 1563–1566; b) D. L. Scott, S. P. White, Z. Otwinowski, W. Yuan, M. H. Gelb, P. B. Sigler, *Science* **1990**, *250*, 1541–1546.

---

Received: February 6, 2002 [F 359]